Kinematic Analysis and Design Optimization for a Reduced-DoF Quadruped Robot with Minimal Torque Requirements

Jingwen Zhang[1], Junjie Shen[1], and Dennis W Hong[1]

***Abstract*— With a unique kinematic arrangement, a new type of quadruped robot with reduced degrees of freedom (DoF) requires minimal-torque actuators to achieve high-payload locomotion. This paper focuses on the kinematic analysis and design optimization for robots of this type. To plan and control its change of posture, a necessary strategy to find feasible solutions of full-body inverse kinematics under additional kinematic constraints is introduced. A design method via nonlinear programming (NLP) is first presented in order to optimize link parameters with guarantee to a series of successive steps. Workspace is also investigated to prepare for further dynamic motion planning. We have verified feasibility of proposed methods with software simulations and hardware implementations, *e.g.*, omni-directional walking and situ rotation.**

I. INTRODUCTION

In recent years, there has been a large surge in research on legged robots. Unlike bipedal robots, quadruped robots are statically stable and don't require active balancing at all times. This helps quadruped robots operate better in human environments. Several emerging quadruped robots, including MIT Cheetah [1] [2], ANYmal [3], SpotMini [4] and Ghost Vision 60 [5], have shown that they can move at a speed comparable to human walking or jogging and handle various terrains such as uneven surfaces and steps. Almost all of those quadruped robots have similar kinematic configurations: each leg has 3 active joints with the same arrangement of rotation axes. Robots with many DoF indeed improve capabilities in navigation and even manipulation. However, this makes robots heavy and imposes high torque requirements on actuators. At the same time, actuators must constantly support the weight of robots even when robots are standing statically which can cause heating problems related to energy loss. Therefore, if quadruped robots with comparable abilities can be constructed with reduced-DoF, it can help bring legged robots closer to assisting human's life.

Different strategies to reduce DoF in legged robots have been developed in the past decades. Quadruped robots with reduced DoF have been constructed in [6], [7] and [8]. Through basic considerations on locomotion requirements, they successfully reduce the required number of DoF to five and even four. However, those robots are not able to select foot placement freely which is important for omni-directional walking and turning. The wheel-legged hybrid configuration is introduced in the RHex [9] which is actually a hexapod robot. [10] applied this principle into a quadruped platform, Quattroped. And [11] and [5] introduce Minitaur with 8 DoF using linkage design. Theoretically, they can handle foot placement with 4 DoF via commanding differential pace on each side. Furthermore those robots are more dynamic due to the capability of leaping. However, the drawback of the design is that actuators of the robot have to support its own weight all the time and this issue still remains unsolved.

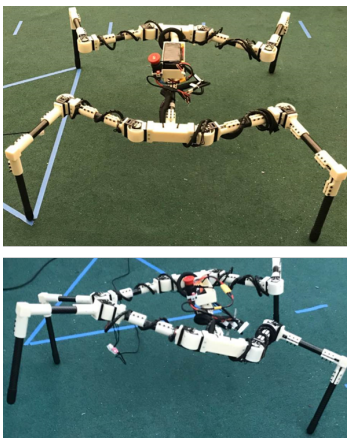

Fig. 1: On the top is the standing pose of the lightweight quadruped robot with reduced DoF. On the bottom is the verification of quasi-static crawling gait.

For a traditional quadruped robot, the reason that actuators must hold its weight is that rotation axes of the hip and knee joints are parallel to the supporting ground at most times. If the direction of axis can be changed to perpendicular with respect to the ground, the weight will be supported by its structure instead of actuators on those joints. Inspired by this idea, in [6], a novel quadruped robot with 9 DoF, 2 per leg and 1 on its body, is first proposed. However, it only briefly touches robots of this kind and leaves many problems unsolved, such as "what is the optimal ratio between links to achieve walking?" and "in order to plan and control the robot's posture changes, how could one solve kinematics efficiently?".

In the following, this paper presents feasible solutions to those problems. Unlike traditional quadruped robots, no redundancy due to reduced DoF adds complexity to full-body inverse kinematics, where virtual 6-DoF of a floating base, generally referred to the robot's body must be included besides controllable joint angles. The additional physical constraints from unique leg configurations are written explicitly, and detailed derivation to feasible solutions of full-

[1]Robotics and Mechanisms Laboratory (RoMeLa), Department of Mechanical and Aerospace Engineering, University of California Los Angeles, CA 90095. zhjwzhang@g.ucla.edu, junjieshen@ucla.edu, dennishong@ucla.edu

body inverse kinematics is provided at the beginning of this paper. Imagine three legs are fixed to the ground through a ball joint, the robot must place its center of mass (CoM) inside the support polygon formed by those grounded legs in order to lift the remaining leg as shown in Fig. 1. To achieve stable quasi-static gaits, the position of CoM must be chosen selectively to accomplish a series of steps. With this requirement, we then formulate design optimization as a nonlinear programming (NLP) problem. Stride length is optimized under guarantee of stable motions while possible degeneration of mobility is avoided via evaluating the condition number of the leg's Jacobian matrix. Based on the proposed method, we simulate and construct a quadruped robot of this kind and experimentally demonstrate its performance in simple locomotion tasks. Body workspace is also investigated to get insights into further motion planning framework to achieve more complex tasks, such as climbing stairs and obstacle avoidance. This paper makes the following contributions:

1) **Kinematics**: A mathematical model of full-body inverse kinematics and body workspace for robots of this kind are investigated. Those prepare the robot for basic locomotion control and advanced motion planning.
2) **Design**: An NLP framework provides a comprehensive guidance to design robots of this kind.
3) **Platform**: An experimental quadruped robot with reduced DoF is constructed following the proposed design method for demonstration on locomotion tasks.

II. KINEMATIC ANALYSIS

This section defines link parameters of the proposed quadruped robot, which are the main variables of design optimization introduced in the Sec. III, and investigates full-body inverse kinematics. The analysis of forward and inverse kinematics for one single leg is trivial in our case where each leg can be treated as a general planar 2R manipulator with one shared revolute joint on its body, therefore it is not discussed in detail in this paper.

A. Kinematic Configuration

Link parameters and coordinate systems are defined following the Denavit-Hartenberg's convention [12] in Fig. 2 where $d_1 \in \mathbb{R}_+$ and $a_1 \in \mathbb{R}_+$ denote half of the body width and body length, $(a_2,\ a_3) \in \mathbb{R}^2_+$ describe the leg length, and $d_4 \in \mathbb{R}_+$ denotes the leg height. The geometrical center of body is chosen as the origin of the body frame (X_b-Y_b-Z_b) for following analysis in this paper. Table I shows the Denavit–Hartenberg parameters (D-H parameters) of the right front leg where α is the link twist, a is the link length, d is the link offset and θ is the joint angle. For other legs, only directions of d_1, a_1, a_2, a_3 need to be changed accordingly *e.g.*, $-d_1$, $-a_1$, $-a_2$, $-a_3$ will be used for the left rear leg. The most essential design goal is to optimize d_1, a_1, a_2, a_3 and d_4 in order to meet mobility requirements.

B. Full-body Inverse Kinematics

For a traditional quadruped robot with 3 DoF per leg, introducing reachability constraints and joint limitations is already sufficient to find feasible solutions to full-body inverse kinematics during footstep planning. Given desired toe positions, the body pose (positions and orientations) can be chosen wisely inside kinematically feasible region with some optimization objectives, *e.g.*, stability and obstacle avoidance [13]. However, additional constraints to kinematically feasible region of the body need to be considered for our proposed quadruped robot in terms of reduced DoF. The additional constraints are due to correlation between the body position and orientation. This section mainly tackles coupled body pose and provides an analytical strategy to find feasible solutions for full-body inverse kinematics.

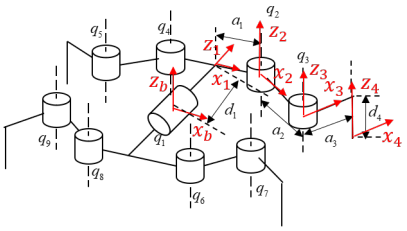

Fig. 2: The illustration of coordinate frames (red), link parameters and joint definitions (black). The picture only shows the example of the right front leg for reference.

TABLE I: D-H parameters for the right front leg

i	α	a	d	θ
1	-90°	0	d_1	q_1
2	90°	a_1	0	q_2
3	0	a_2	0	q_3
4	0	a_3	$-d_4$	0

For convenience, the following notation rules are used in this paper: 1) subscripts are used to index the origin of a frame while superscripts are used to denote the observational reference frame, *e.g.*, ${}^w\mathbf{P}_b$ denotes the origin of the body frame with respect to the world frame. 2) $\mathbf{P}$ is used to describe 3-dimensional position vector while $\mathbf{x}$, $\mathbf{y}$, and $\mathbf{z}$ are used to denote unit vector along x, y, and z axes respectively. 3) $\mathbf{R}_x$, $\mathbf{R}_y$, and $\mathbf{R}_z$ stands for rotation maxtrix around x, y, and z axes respectively. 4) $c\alpha = \cos(\alpha)$, $s\alpha = \sin(\alpha)$.

For a floating-base robotic system, the floating base, generally referred to the body of the robot, introduces extra 6 DoF to make it underactuated. We can describe the body pose as (${}^w\mathbf{P}_b$, ${}^w\mathbf{R}_b$) and the transformation of toe positions from the world frame to the body frame can be accomplished via:

$$ {}^b\mathbf{P}_i = {}^w\mathbf{R}_b^T({}^w\mathbf{P}_i - {}^w\mathbf{P}_b), \tag{1} $$

where i is the leg index ($i = 1,2,3,4$ for our case). After obtaining toe positions with respect to the body frame, inverse kinematics for each single leg is applied to find joint angles $\mathbf{q}$. Thus, full-body inverse kinematics requires knowledge of the body position ${}^w\mathbf{P}_b$ and orientation expressed as ${}^w\mathbf{R}_b$.

All 6 DoF of the body can be pre-planned for traditional quadruped robots while our proposed robot, in general, can only plan 3 of them in advance and another 3 need to be determined accordingly. For example, suppose the toe

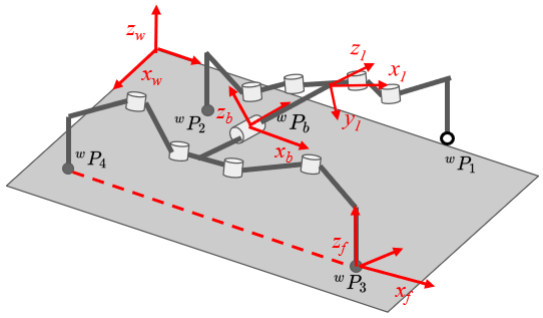

Fig. 3: The illustration of important robot coordinates including the world frame (X_w-Y_w-Z_w), the body frame (X_b-Y_b-Z_b), the toe frame (X_f-Y_f-Z_f) and the frame of the front-end body (X_1-Y_1-Z_1) which is the same joint frame of body waist as shown in Fig. 2.

positions relative to the world frame, ${}^w\mathbf{P}_1$, ${}^w\mathbf{P}_2$, ${}^w\mathbf{P}_3$, ${}^w\mathbf{P}_4$ are known and they are reachable given the position of the body ${}^w\mathbf{P}_b$ in Fig 3. Here ${}^w\mathbf{P}_b \in \mathbb{R}^3$ are picked as known parameters to find the other 3 orientation values which can also be expressed as a rotation matrix relative to the world frame ${}^w\mathbf{R}_b$. By observation, ${}^w\mathbf{R}_b$ can be decomposed as

$$ {}^w\mathbf{R}_b = [{}^w\mathbf{x}_b \ {}^w\mathbf{y}_b \ {}^w\mathbf{z}_b] = {}^w\mathbf{R}_f \cdot \mathbf{R}_x(\alpha) \cdot \mathbf{R}_z(\gamma). \tag{2} $$

Given ${}^w\mathbf{P}_4$ and ${}^w\mathbf{P}_3$, the rotation matrix ${}^w\mathbf{R}_f = [{}^w\mathbf{x}_f \ {}^w\mathbf{y}_f \ {}^w\mathbf{z}_f]$ from the toe frame (X_f-Y_f-Z_f) to the world frame (X_w-Y_w-Z_w) can be treated as known parameter. From the toe frame (X_f-Y_f-Z_f) to the body frame (X_b-Y_b-Z_b), roll angle α and yaw angle γ between those two frames need to be determined. By further observation, the distance between the body and each toe along each corresponding z_4-axis always equals to the leg height d_4, which creates additional constraints as follows:

$$ \begin{cases} {}^w\mathbf{z}_b^T {}^w\mathbf{P}_{b3} = d_4 \\ {}^w\mathbf{z}_b^T {}^w\mathbf{P}_{b4} = d_4 \\ -{}^w\mathbf{y}_1^T {}^w\mathbf{P}_{b1} = d_4 \\ -{}^w\mathbf{y}_1^T {}^w\mathbf{P}_{b2} = d_4 \end{cases}, \tag{3} $$

where ${}^w\mathbf{P}_{bi} = {}^w\mathbf{P}_b - {}^w\mathbf{P}_i \ (i = 1,2,3,4)$. The unit vector ${}^w\mathbf{z}_b$ in constraint (3) can be found from

$$ [\sim \ \sim \ {}^w\mathbf{z}_b] = {}^w\mathbf{R}_f \cdot \mathbf{R}_x(\alpha) \tag{4} $$

as

$$ {}^w\mathbf{z}_b = {}^w\mathbf{z}_f \cdot \cos(\alpha) - {}^w\mathbf{y}_f \cdot \sin(\alpha) \tag{5} $$

Then we can obtain α by substituting (5) into the first equation of constraint (3) as follows:

$$ ({}^w\mathbf{z}_f^T {}^w\mathbf{P}_{b3})\cos(\alpha) + (-{}^w\mathbf{y}_f^T {}^w\mathbf{P}_{b3})\sin(\alpha) = d_4 \tag{6} $$

As for γ, the unit vector ${}^w\mathbf{y}_1$ in constraint (3) can be found from

$$ [{}^w\mathbf{x}_1 \ {}^w\mathbf{y}_1 \ {}^w\mathbf{z}_1] = {}^w\mathbf{R}_1 = {}^w\mathbf{R}_b \cdot \mathbf{R}_x(-90^\circ) \cdot \mathbf{R}_z(q_1) \tag{7} $$

as

$$ {}^w\mathbf{y}_1 = -{}^w\mathbf{x}_b \cdot \sin(q_1) - {}^w\mathbf{z}_b \cdot \cos(q_1), \tag{8} $$

where q_1 is the joint angle of body waist and

$$ \begin{cases} {}^w\mathbf{x}_b = {}^w\mathbf{x}_f c\gamma + ({}^w\mathbf{y}_f c\alpha + {}^w\mathbf{z}_f s\alpha)s\gamma \\ {}^w\mathbf{z}_b = {}^w\mathbf{z}_f c\alpha - {}^w\mathbf{y}_f s\alpha \end{cases}. \tag{9} $$

Substitute ${}^w\mathbf{y}_1$ expressed as equation (8) into the third and fourth equations of constraint (3) with a coordinate transformation as follows:

$$ \begin{bmatrix} \bar{x} \\ \bar{y} \\ \bar{z} \end{bmatrix} = \begin{bmatrix} c\gamma s q_1 \\ s\gamma s q_1 \\ c q_1 \end{bmatrix} \tag{10} $$

The equation constraints can then be written explicitly as follows where γ and q_1 can be found analytically:

$$ \begin{cases} g_1\bar{x} + g_2\bar{y} + g_3\bar{z} = d_4 \\ g_4\bar{x} + g_5\bar{y} + g_6\bar{z} = d_4 \\ \bar{x}^2 + \bar{y}^2 + \bar{z}^2 = 1 \end{cases}, \tag{11} $$

where

$$ \begin{cases} g_1 = {}^w\mathbf{x}_f^T {}^w\mathbf{P}_{b1} \\ g_2 = ({}^w\mathbf{y}_f^T c\alpha + {}^w\mathbf{z}_f^T s\alpha) {}^w\mathbf{P}_{b1} \\ g_3 = ({}^w\mathbf{z}_f^T c\alpha - {}^w\mathbf{y}_f^T s\alpha) {}^w\mathbf{P}_{b1} \\ g_4 = {}^w\mathbf{x}_f^T {}^w\mathbf{P}_{b2} \\ g_5 = ({}^w\mathbf{y}_f^T c\alpha + {}^w\mathbf{z}_f^T s\alpha) {}^w\mathbf{P}_{b2} \\ g_6 = ({}^w\mathbf{z}_f^T c\alpha - {}^w\mathbf{y}_f^T s\alpha) {}^w\mathbf{P}_{b2} \end{cases}. \tag{12} $$

After obtaining α and γ, we can find ${}^w\mathbf{R}_b$ from equation (2). With ${}^w\mathbf{R}_b$ and ${}^w\mathbf{P}_b$ determined, equation (1) and single leg inverse kinematics can be applied to compute joint angles $\mathbf{q}$ given toe positions ${}^b\mathbf{P}_i \ (i = 1,2,3,4)$. Meanwhile, constraint (3) provides necessary additional kinematic constraints that motion planners have to consider by no means in order to find feasible trajectories. The singularity happens when $\alpha = 0$, which indicates all the four toes are actually in the same plane ($q_1 = 0$). In that case, any choice of γ within a certain range becomes feasible.

III. DESIGN OPTIMIZATION

The key goal of this research is to investigate how the design parameters, such as the leg length and height, could be determined to create optimal steps. In order to optimize the model shown in Fig 2, five basic parameters, half of the body length d_1, half of the body width a_1, leg lengths a_2 and a_3, and leg height d_4, could be optimized. Due to too many uncertainties for the design process, including stepsize of a single step, initial postures and mass distributions, it is intractable to optimize parameters one by one via creating analytical relationship between one individual parameter and optimization objectives. Instead, we use nonlinear programming (NLP) to formulate one single optimization problem under appropriate constraints.

In order to reduce the number of parameters to be optimized, d_1 is chosen as the reference parameter ($d_1 = 1$ for

simplification) while the problem is to find optimal ratios of target variables to d_1. We choose to solve this problem in such way since the real robot size could be determined afterwards by choosing specific value for d_1 without losing generality. However, NLP solvers are sometimes struggling with local optima without global optimality guarantee. To mitigate this problem, we put efforts to analyze optimized results to check whether they make physical meaning or not and create better initial guess accordingly. The choice of leg height d_4 is analyzed alone afterwards using full-body inverse kinematics such that the NLP problem can be further simplified as a planar problem.

A. Leg Lengths and Body Width

Based on the walking strategy described in Sec. I, two correlated considerations concerning the optimization of the leg length and body width are presented as 1) planar workspace of the body and 2) stability of the motion. For quasi-static gaits, in order to lift one leg via rotating body waist q_1, we need to make sure its CoM is inside the supporting triangle formed by the other grounded legs. If we assume mass-less links for legs, the body movement will play a leading role of moving its CoM. In addition, large body workspace will give us more freedom to generate stable motions. With this fundamental premise, stride length Δd is taken as the main objective function to be optimized when only a naive straight walking strategy with zero yaw angle is considered here.

Based on the unique kinematic arrangement, the model could become a 4-RRR planar parallel manipulator when the angle of body waist q_1 is zero and fixed toe positions are assumed, design criteria for parallel manipulators to render the largest workspace are taken into considerations here [14] [15] [16], 1) Equal length of links (leg lengths a_2 and a_3 in our case) given total length of two links; 2) Increase link lengths and decrease platform size (body size a_1 and d_1 in our case). The first criterion is accepted as one of the constraints as follows:

$$a_2 = a_3 \tag{13}$$

Meanwhile, to avoid interference between the front legs and rear legs, the following constraint needs to be satisfied:

$$a_2 \leq d_1 \tag{14}$$

The following part formulates the second criterion as an NLP. Under the constraint of stability, we need to answer questions, such as "**how large could we make a_2 and a_3?**" and "**by how much could we decrease a_1 given d_1?**". Besides those link parameters $\mathbf{k} = [a_1, a_2, a_3, d_1]^T \in \mathbb{R}^4$, decision variables also consider the leg configuration via leg joints $\mathbf{q}_{leg} = [q_i | i = 2, \ldots, 9]$, the initial posture which is expressed by a square with side length l as shown in Fig 4 for simplification, the stride length Δd and forward displacement of the body center Δx. In this planar problem, it is trivial to compute the x-y plane projection of its CoM as $\mathbf{P}_{CoM} = f(\mathbf{k}, \mathbf{q}_{leg}, \Delta d)$ with point mass on each joint assuming mass-less links, the stability constraint can be written as:

$$\mathbf{P}_{CoM} \in \{\mathbf{x} \in \mathbb{R}^2 | \mathbf{A}_s \mathbf{x} \leq \mathbf{b}_s\}, \tag{15}$$

where $\mathbf{A}_s$ and $\mathbf{b}_s$ denote the convex supporting polygon which is a triangle computed from toe positions of the other three grounded legs. In terms of cost function, the stride length Δd is introduced as main goal of optimization, and the condition number of leg Jacobian matrix $\mathbf{J}(\mathbf{q}_{leg})$ is combined to avoid singular leg configurations. With additional physical constraints including joint limits and forward kinematics, the entire NLP problem is formulated as follows:

$$\begin{aligned}
\underset{\mathbf{k},\ \mathbf{q}_{leg},\ l,\ \Delta d,\ \Delta x}{\text{minimize}} \quad & -\Delta d + w \cdot cond\left(\mathbf{J}(\mathbf{q}_{leg})\right) \\
\text{subject to} \quad & \mathbf{A}_s \mathbf{P}_{CoM} \leq \mathbf{b}_s \\
& a_2 = a_3 \\
& a_2 \leq d_1 \\
& \mathbf{k}_{min} \leq \mathbf{k} \leq \mathbf{k}_{max} \\
& \mathbf{q}_{min} \leq \mathbf{q}_{leg} \leq \mathbf{q}_{max} \\
& \begin{bmatrix} f_{FK}^1 \\ f_{FK}^2 \\ f_{FK}^3 \\ f_{FK}^4 \end{bmatrix} = \begin{bmatrix} \Delta x + \Delta d + l/2 & l/2 \\ \Delta x + l/2 & -l/2 \\ \Delta x - l/2 & l/2 \\ \Delta x - l/2 & -l/2 \end{bmatrix}
\end{aligned},$$

where $\mathbf{k}_{min}, \mathbf{k}_{max} \in \mathbb{R}^4$ describe link parameters physical boundary, *e.g.*, mechanical implementation related to motor sizes, $\mathbf{q}_{min}, \mathbf{q}_{max} \in \mathbb{R}^8$ denote joint limits and $f_{FK}^i(\cdot)$ is the forward kinematics function based on Table I used to compute toe position (x_i, y_i) of leg i. In the cost function, $cond(\cdot)$ computes the condition number of the Jacobian matrix, w is the weight used to tune the optimizer.

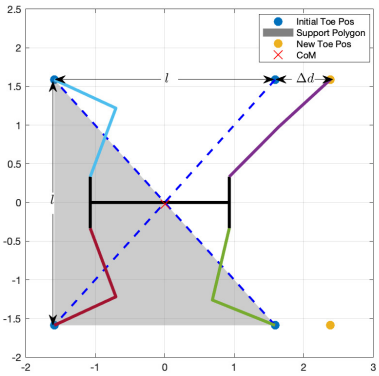

Fig. 4: MATLAB visualization of NLP optimized result. Blue dots denote initial toe positions while yellow dots denote desired new positions for the swing leg. The result shows CoM (red cross) is optimized near the edge of the support polygon (shaded) to maximize stride length Δd.

According to our setup of the NLP optimization problem, it could be solved efficiently using many commercial solvers. The optimized result is visualized via MATLAB in Fig 4 for qualitative analysis while the detailed quantitative result is presented in Sec. IV. The result answers the two proposed questions since it shows:

1) In order to increase the stride length, the leg link length a_2 and a_3 are increased. Without violating the stability of moving forward quasi-statically, its CoM is already pushed to the boundary of the supporting triangle in Fig. 4. And the swing leg is fully extended to maximize the forward distance.
2) Given leg length and body length, a_1 concerning the body width is decreased to render a larger body workspace. In Fig. 4, if a_1 is decreased further, Jacobian matrix will tell us that three grounded legs will be closer to singularity, which could cause unexpected issues to following steps.

B. Leg Height

Given the body length and leg link lengths, the leg height d_4 is the only remaining parameter to be optimized. It affects reachable heights of both the robot's toe and body via limiting the maximum angle that its body could rotate, in other words, the maximum value of body waist q_1. Imaging having an infinite height for legs, the robot could not rotate the body at all. To verify this intuition and show the relation between them, full-body inverse kinematics described in Sec. II-B is used to find the maximum value for q_1 that has a feasible solution and then maximum reachable height of the toe and body could be determined. Fig. 5 is obtained by sweeping possible values for d_4. To be consistent, relative leg height, defined as the ratio of d_4 to d_1 is used.

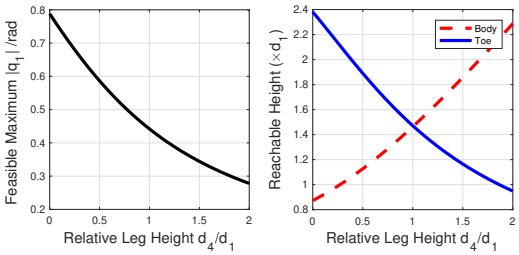

Fig. 5: On the left is the relationship between the relative leg height and maximum body waist q_1 with feasible inverse kinematics solution. On the right shows maximum reachable height of the body and toe with respect to relative leg height.

Fig. 5 shows that maximum value for q_1 is indeed decreasing as relative leg height increases and will converge to zero eventually that matches with our physical intuition. On the right of Fig. 5 proposes a tradeoff between the maximum heights of the robot's toe and body. With large relative leg height, its body is kept far away from the ground. However, due to small allowed rotation of its body, the leg can only be lifted for a small amount which causes the toe height decreasing. This is useful to decide the optimal value of leg height d_4 according to application requirements, *e.g.*, standard step height.

IV. RESULTS

A. Robotic Platform

Following the optimization result visualized in Fig. 4, optimal ratios are obtained as $a_1/d_1 = 0.3332$, $a_2/d_1 = 0.9599$ and $a_3/d_1 = 0.9599$ with weight $w = 1.2$. We pick d_1 as $300mm$ and a_1 can be designed as around $100mm$ accordingly. a_2 and a_3 should be determined as $287.98mm$. However, the final value is $270mm$ due to motor housing that requires more room to avoid interference. In terms of the leg height d_4, in order to achieve enough heights for both the body and toes, the relative leg height is picked as 0.95 so that $d_4 = 285mm$. Links of body and legs mainly consist of carbon fiber tubes in order to provide enough strength to support the weight. Motors are chosen as Dynamixel XM540 and motor housings are built via 3D-printing. Toes are covered by anti-slip tubes to enhance friction. The parameters are summarized in Table II.

TABLE II: Robot Configuration

Parameter	Value
Total Degrees of Freedom	9
Body Height	283 [mm]
Body Size	600 × 200 [mm]
Leg Length (fully extended)	540 [mm]
Total Weight	5.3 [kg]
Stall Torque of Each Motor	12.9 [Nm]

The payload the robot can withstand is highly dependent on the link material and the quality of motor housings. Although this 3D-printed prototype as shown in Fig. 1 is unable to provide empirical payload info about robots with this design, it helps investigate and verify the motion analysis. After moving its body to one side, the robot can stand stable with 3 legs on the ground which is the basic requirement for quasi-static gaits implementation.

B. Body Workspace

In order to prepare for complicated locomotion tasks, *e.g.*, dynamic trotting and step climbing, the body workspace is necessary to plan the motion of CoM. Given the feasible toe positions, the analysis of body workspace begins with a special planar case where four toes are on the same plane. Afterwards, it is extended to the more general case in three dimensions (3D).

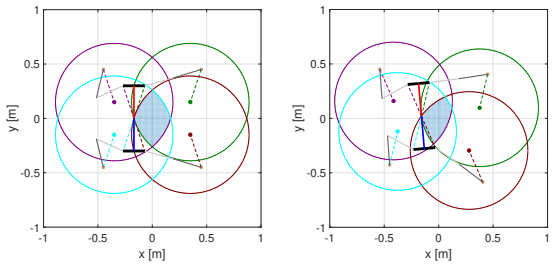

Fig. 6: Planar body workspace (blue area) with fixed yaw angle γ. For the left example, $\gamma = 0^\circ$ and the toe positions are the NLP optimization results. For the right example, the yaw angle $\gamma = 5^\circ$ and different initial toe positions. One critical configuration of the robot is also plotted for demonstration when the body is on the edge of its workspace.

1) The Planar Case: When body waist $q_1 = 0$, four legs stand on the same plane which is the case for movements on the ground. Without loss of generality, the plane $z = 0$ is chosen for simplicity. If the yaw angle γ is further fixed, constant orientation workspace of body is defined as the intersection region of four circles as shown in Fig. 6. The center of each circle is shifted from its corresponding toe position by the same amount from each shoulder to the body, as illustrated by the dashed lines in Fig. 6. The radius r of each circle is the fully-extended leg length, *i.e.*, $r = a_2 + a_3$. The planar body workspace Ω with fixed yaw angle can thus be defined analytically as follows:

$$\begin{aligned}\Omega = \{\, [x,y,z]^T \in \mathbb{R}^3 \mid\ & z = d_4, \\ & \left\| [x,y,0]^T - {}^w\mathbf{P}_i + {}^w\mathbf{P}_{bs_i} \right\| \le r,\ i = 1,2,3,4 \,\},\end{aligned} \tag{16}$$

where ${}^w\mathbf{P}_{bs_i} = \mathbf{R}_z(\gamma)\,[a_{1i},\ d_{1i},\ 0]^T$ is the position vector from the body to the i^{th} shoulder in the world frame, and a_{1i} and d_{1i} are the corresponding D-H parameters for the i^{th} leg. The extreme values for γ can also be determined numerically by gradually increasing or decreasing γ until Ω becomes a single point. In other words, there are two circles tangent to each other geometrically as shown in Fig. 7 and the workspace degenerates to the tangent point. To go a step further, the complete planar body workspace can be obtained collectively with all feasible yaw angles, as shown in Fig. 8. The shape is very likely to be an ellipse, which is worth studying in the future.

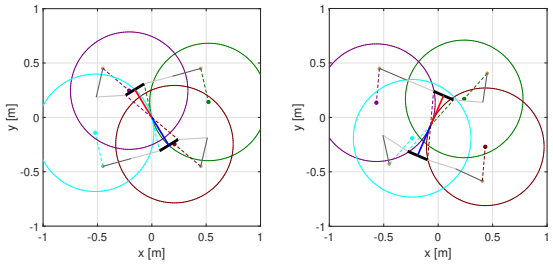

Fig. 7: Given toe positions on the left, configuration of robot is plotted with the largest yaw angle $\gamma = 31.4°$ within the feasible range $-31.4° \le \gamma \le 31.4°$. On the right, the smallest $\gamma = -23.4°$ is picked with feasible range $-23.4° \le \gamma \le 32.8°$ given different toe positions.

2) The 3D Case: To be more general, the case $q_1 \neq 0$ is considered when four toes are not on the same plane. The analysis of body workspace becomes extremely challenging and it seems that there is no simple analytical solution. Therefore, the 3D body workspace is obtained numerically by examining whether the solution of inverse kinematics exists. More specifically, we firstly realize that if the body orientation, *i.e.*, roll and yaw angles α, γ are fixed and feasible, the body workspace is a line segment, as suggested by constraint (3). Therefore, we can alternatively pick one of α, γ, and z_b as known parameter and solve for the other two. With investigation on all feasible α and z_b, the 3D body workspace with fixed yaw angle is shown in the left column of Fig. 9. The toe positions are given by the NLP optimization results described in Sec. III while the right front leg is lifted 150 mm. The body workspace is a curved surface like a potato chip, similar to the planar case but with a certain distortion. Similarly, the complete body workspace can be also obtained by sweeping all feasible yaw angles, as shown in the right column of Fig. 9. It spans a larger thickness while the project on X-Y plane is also similar to the planar case.

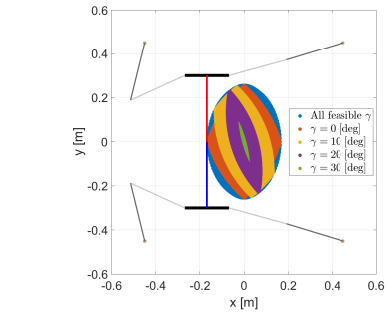

Fig. 8: Complete planar body workspace considering all feasible yaw angles, *e.g.*, the orange area, corresponding to $\gamma = 0$ deg, is the same as the left example in Fig. 6.

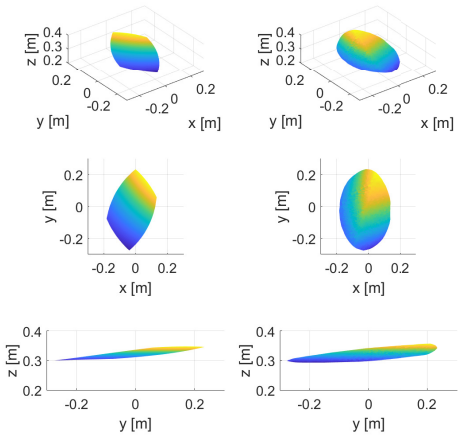

Fig. 9: On the left are different views of the 3D body workspace with yaw angle $\gamma = 0°$. The feasible range of roll angle is $3.1° \le \alpha \le 6.4°$. On the right is the complete 3D body workspace but for all feasible yaw angles $-25.8° \le \gamma \le 34.7°$. The feasible roll angle is $1.5° \le \alpha \le 7.0°$.

C. Quasi-static Gait Implementation

From the result of design optimization, we can observe that CoM is almost on the edge of the supporting triangle in Fig. 4 when the largest stride is achieved, which is dangerous for hardware implementation. Instead of moving body simply forwards or backwards, the smarter way is to move body in the direction normal to the edge that can help CoM stay away from that edge. The simulation is shown in Fig 10.

The simulation strategy is implemented in the hardware to accomplish locomotion tasks. Positions, velocities and

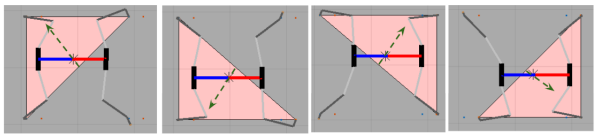

Fig. 10: From left to the right is the sequence of selectively lifting the leg with moving the CoM in the direction normal to the edge of the supporting triangle. The pink area indicates the instant supporting triangle formed by three grounded legs. The green arrow indicates the body moving direction.

accelerations of desired joint angles along a sequence of quasi-static postures are commanded into a feedforward PID controller to follow desired motion trajectory. Forward and backward walking can be achieved and additionally it works well for side-walking and situ rotation where only discrete quasi-static postures need to be re-planned. The hardware implementation is shown in Fig. 11 and the full demonstration can be viewed in the accompanied video (https://youtu.be/r-OWLAW6yp0).

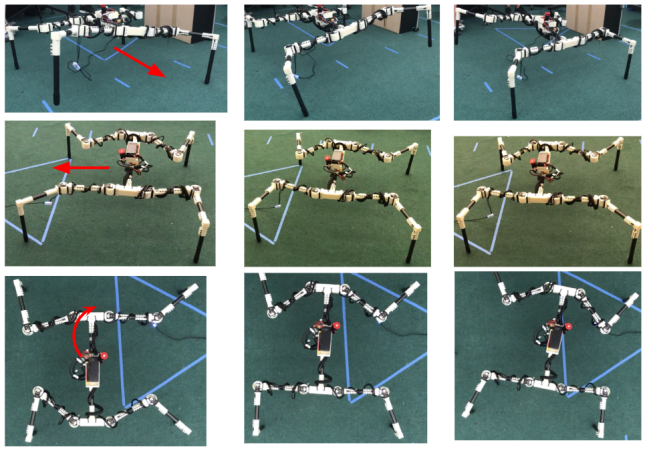

Fig. 11: Screen shots of the hardware implementation. On the top is a step forward, in the middle is the side walking to the left and on the bottom is the robot in situ rotation.

V. CONCLUSIONS & FUTURE WORKS

This paper provides the first complete guidance concerning designing robots of any size with a special DoF configuration. The design problem is formulated as an NLP problem. Although the global optimality is not guaranteed, qualitative analysis of the optimized result is done to make sure the NLP gives us reasonable and interpretable design guidance. We verify feasibility of this design optimization with software simulations and hardware implementations. A mathematical model of full-body inverse kinematics for robots of this kind is discussed. New kinematic constraints due to reduced DoF are adopted to solve the problem with coupled position and orientation of the floating base.

The detailed body workspace is analyzed and several possible constraints on CoM are introduced in order to prepare this robot for motion planning. 3D body workspace is really useful for step climbing since the body is not moving in a horizontal plane anymore. And from the observation of our experiments, the robot sometimes lifts the diagonal legs simultaneously leading to a failure. We speculate that the CoM is misplaced exactly on the diagonal line due to tracking errors of the CoM trajectory which needs further investigation. However, this indicates robots with this design have potentials to achieve dynamic trotting. Meanwhile, the use of transmission mechanism on one single leg can reduce the inertia a lot in order to achieve faster motions since the leg motors are not supporting the weight.

REFERENCES

[1] G. Bledt, M. J. Powell, B. Katz, J. Di Carlo, P. M. Wensing, and S. Kim, "Mit cheetah 3: Design and control of a robust, dynamic quadruped robot," in *2018 IEEE/RSJ International Conference on Intelligent Robots and Systems (IROS)*, pp. 2245–2252, IEEE, 2018.

[2] P. M. Wensing, A. Wang, S. Seok, D. Otten, J. Lang, and S. Kim, "Proprioceptive actuator design in the mit cheetah: Impact mitigation and high-bandwidth physical interaction for dynamic legged robots," *IEEE Transactions on Robotics*, vol. 33, no. 3, pp. 509–522, 2017.

[3] M. Hutter, C. Gehring, D. Jud, A. Lauber, C. D. Bellicoso, V. Tsounis, J. Hwangbo, K. Bodie, P. Fankhauser, M. Bloesch, *et al.*, "Anymal-a highly mobile and dynamic quadrupedal robot," in *2016 IEEE/RSJ International Conference on Intelligent Robots and Systems (IROS)*, pp. 38–44, IEEE, 2016.

[4] E. Ackerman, "Boston dynamics' spotmini is all electric, agile, and has a capable face-arm," 2016.

[5] "Ghost robotics," *https://www.ghostrobotics.io*.

[6] K. Yoneda, Y. Ota, F. Ito, and S. Hirose, "Construction of a quadruped with reduced degrees of freedom," in *2000 26th Annual Conference of the IEEE Industrial Electronics Society. IECON 2000. 2000 IEEE International Conference on Industrial Electronics, Control and Instrumentation. 21st Century Technologies*, vol. 1, pp. 28–33, IEEE, 2000.

[7] K. Yoneda, "Light weight quadruped with nine actuators," *Journal of Robotics and Mechatronics*, vol. 19, no. 2, pp. 160–165, 2007.

[8] M. Buehler, R. Battaglia, A. Cocosco, G. Hawker, J. Sarkis, and K. Yamazaki, "Scout: A simple quadruped that walks, climbs, and runs," in *Proceedings. 1998 IEEE International Conference on Robotics and Automation (Cat. No. 98CH36146)*, vol. 2, pp. 1707–1712, IEEE, 1998.

[9] U. Saranli, M. Buehler, and D. E. Koditschek, "Rhex: A simple and highly mobile hexapod robot," *The International Journal of Robotics Research*, vol. 20, no. 7, pp. 616–631, 2001.

[10] S.-Y. Shen, C.-H. Li, C.-C. Cheng, J.-C. Lu, S.-F. Wang, and P.-C. Lin, "Design of a leg-wheel hybrid mobile platform," in *2009 IEEE/RSJ International Conference on Intelligent Robots and Systems*, pp. 4682–4687, IEEE, 2009.

[11] G. Kenneally, A. De, and D. E. Koditschek, "Design principles for a family of direct-drive legged robots," *IEEE Robotics and Automation Letters*, vol. 1, no. 2, pp. 900–907, 2016.

[12] R. S. Hartenberg and J. Denavit, "A kinematic notation for lower pair mechanisms based on matrices," *Journal of applied mechanics*, vol. 77, no. 2, pp. 215–221, 1955.

[13] M. Zucker, N. Ratliff, M. Stolle, J. Chestnutt, J. A. Bagnell, C. G. Atkeson, and J. Kuffner, "Optimization and learning for rough terrain legged locomotion," *The International Journal of Robotics Research*, vol. 30, no. 2, pp. 175–191, 2011.

[14] X. Huang, T. Li, B. Xu, and J. Wu, "Parameter design and manufacture for the 4rrr parallel manipulator," in *Proceedings of 2011 International Conference on Electronic & Mechanical Engineering and Information Technology*, vol. 5, pp. 2540–2543, IEEE, 2011.

[15] J.-P. Merlet, C. M. Gosselin, and N. Mouly, "Workspaces of planar parallel manipulators," *Mechanism and Machine Theory*, vol. 33, no. 1-2, pp. 7–20, 1998.

[16] J. Wu, J. Wang, L. Wang, and Z. You, "Performance comparison of three planar 3-dof parallel manipulators with 4-rrr, 3-rrr and 2-rrr structures," *Mechatronics*, vol. 20, no. 4, pp. 510–517, 2010.